Cell Reports, Volume *27*

Supplemental Information

Mucus Architecture and Near-Surface Swimming Affect Distinct *Salmonella* Typhimurium Infection Patterns along the Murine Intestinal Tract

Markus Furter, Mikael E. Sellin, Gunnar C. Hansson, and Wolf-Dietrich Hardt

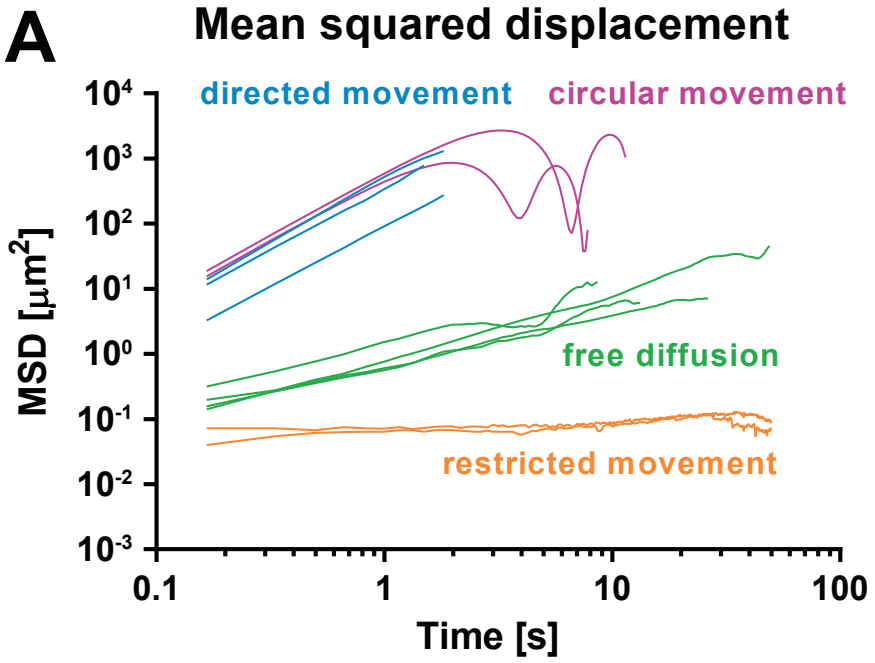
A
Mean squared displacement
directed movement
circular movement
free diffusion
restricted movement
MSD [μm²]
10⁴
10³
10²
10¹
10⁰
10⁻¹
10⁻²
10⁻³
0.1
1
10
100
Time [s]

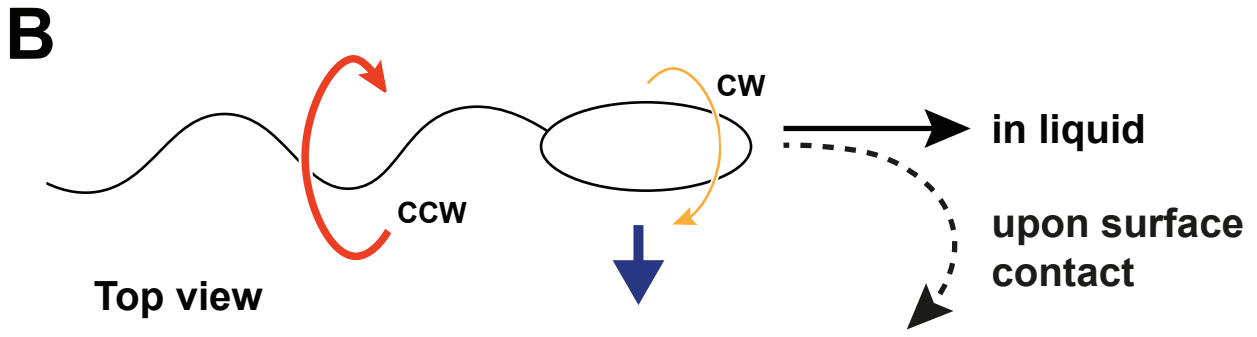
B
CW
CCW
Top view
in liquid
upon surface contact

Fig. S1, related to Fig. 1: Measuring bacterial near surface swimming with the mean squared displacement. (A) The mean squared displacement (MSD) is a way to characterize the random walk of particles in 1 to 3 dimensions. For each time interval possible, the average distance travelled (squared, to avoid negative values) is calculated and plotted on the MSD graph. Particles that are constrained in their movement or move slowly produce a slight slope whereas freely diffusing and actively moving particles have steeper slopes. The circular motion during NSS generates an oscillating curve since the bacterium repeatedly returns to the origin of its trajectory. (B) Schematic drawing of the forces exerted on bacteria during near surface swimming (NSS). The torque of the flagella rotating counter-clockwise (CCW, Red arrow) induces a slower rotation of the bacterial body in the opposite direction (CW, yellow arrow). Upon contact with a surface, the rotation of the bacterial body generates a perpendicular force (blue arrow) that diverts the bacterium from its linear to a circular track.

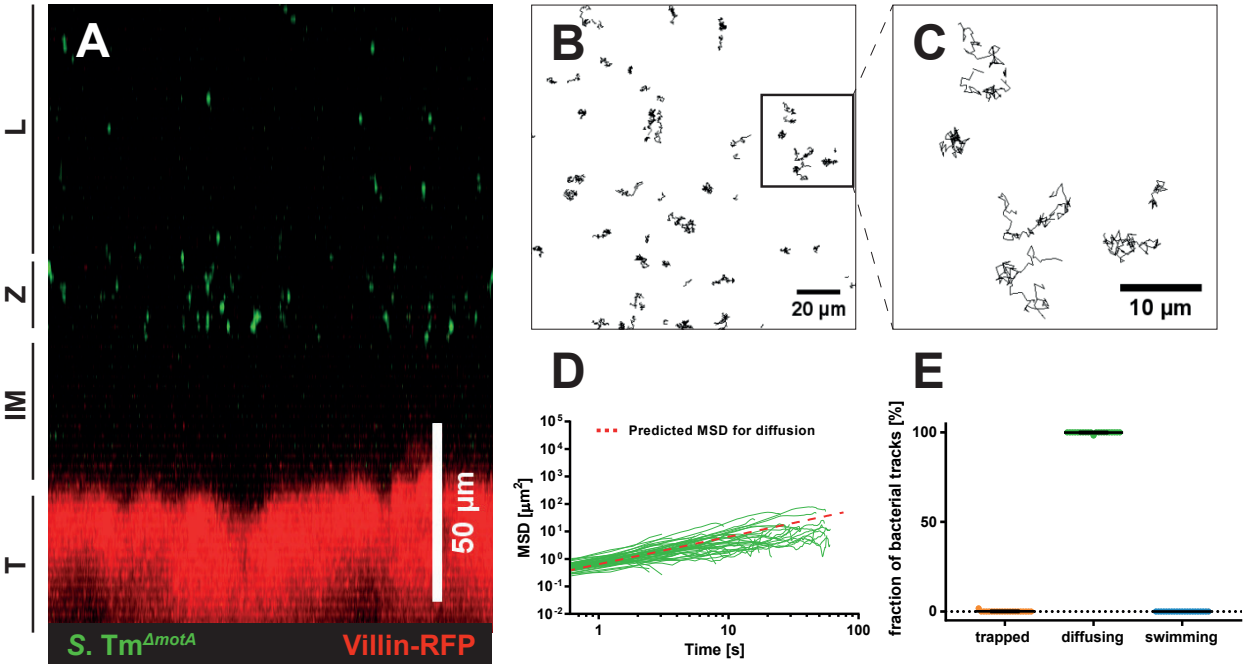
A
L
Z
IM
T
50 µm
S. Tm ΔmotA
Villin-RFP
B
20 µm
C
10 µm
D
Predicted MSD for diffusion
MSD [µm²]
Time [s]
E
fraction of bacterial tracks [%]
trapped
diffusing
swimming

Fig. S2, related to Fig. 2: *S.*Tm$^{\Delta motA}$ is not trapped in the mucus layer. Distal colon tissue samples were excised from untreated *villin-RFP* mice and mounted on a petri dish. After mounting, green fluorescent *S.*Tm were added onto the tissue and confocal image stacks were acquired. (A) Side-view of a confocal z-stack after addition of *S.*Tm$^{\Delta motA}$. The image is labeled as in Fig. 1. (B) Time-lapse imaging of the mucus surface in image stack (A). The tracks of the bacteria on the mucus are shown in black. (C) Magnification of the area marked in (B). (D) Mean Squared Displacement (MSD) calculated from 50 random *S.*Tm$^{\Delta motA}$ tracks at the colon mucus surface. The plot is color-coded for the motility phenotype of each track as in Fig. 1. (E) Trapped, diffusing and swimming *S.*Tm were quantified manually based on optical appearance of the tracks. Depicted is the mean ± SD from three independent experiments.

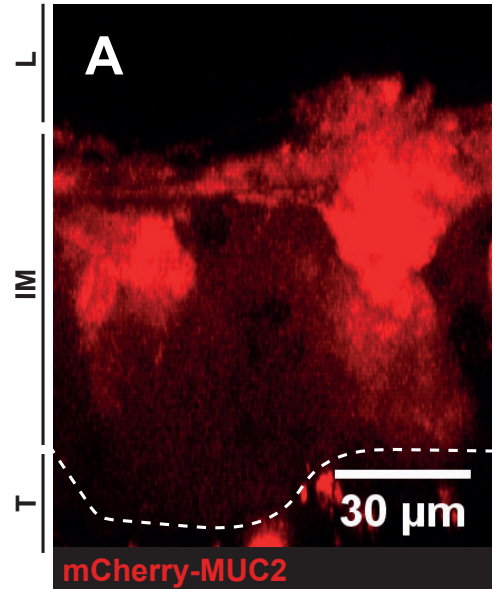
A
L
IM
T
30 µm
mCherry-MUC2

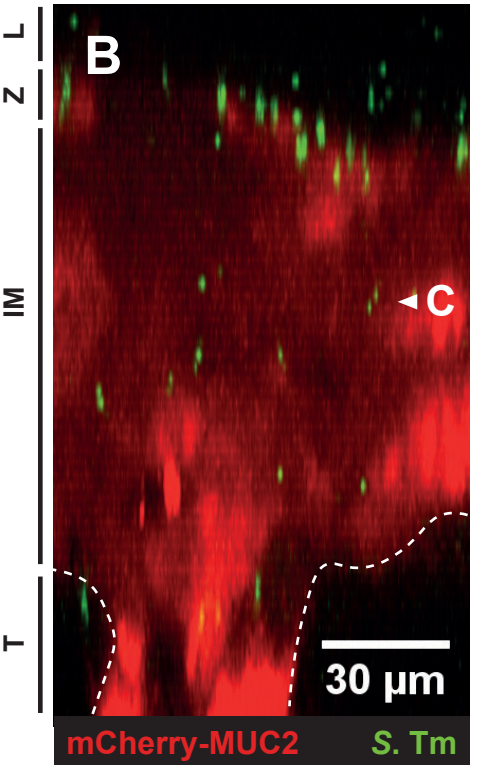
B
L
Z
IM
T
C
30 µm
mCherry-MUC2
S. Tm

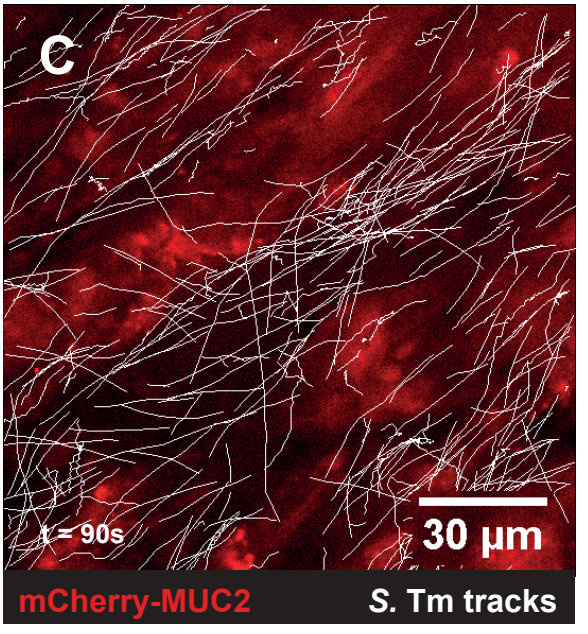
C
t = 90s
30 µm
mCherry-MUC2
S. Tm tracks

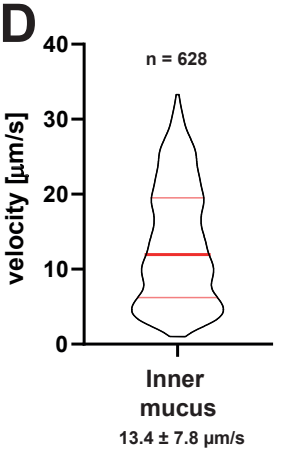
D
n = 628
velocity [µm/s]
40
30
20
10
0
Inner
mucus
13.4 ± 7.8 µm/s

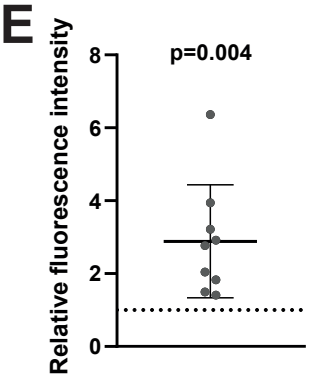
E
p=0.004
Relative fluorescence intensity
8
6
4
2
0

Fig. S3, related to Fig. 4: *S.*Tm can probe for heterogeneities to penetrate the mucus. This proof of principle-type experiment visualizes *S.*Tm interactions with inner mucus layer heterogeneities. For this purpose, we used distal colon explants of *RedMUC2*^{98trTg} mice. These mice show an uneven, aberrant mucus distribution, caused by the presence of both, the native murine Muc2 and mCherry-tagged human MUC2. It is important to note that this heterogeneous mucus does not represent the situation in wild type mice, and is a specific artefact of the *RedMUC2*^{98trTg} mice. (A) Explant imaging of distal colon samples from untreated *RedMUC2*^{98trTg} mice, revealing uneven distribution of the fluorescent signal. It is currently not clear, whether dimly fluorescent areas are enriched with unlabeled, murine mucus or have an overall lower mucus density. Shown is the side-view of a representative confocal z-stack. Labels indicate the tissue (T), inner mucus layer (IM) and the lumen / loose mucus (L). (B-E) Distal colon tissue from untreated *RedMUC2*^{98trTg} mice was infected with *S.*Tm^{GFP}. (B) Side-view of a confocal z-stack after addition of the bacteria. *S.*Tm^{GFP} accumulates on the Z-layer and traverses the mucus in a few cases. (C) Time-lapse imaging of the tissue surface in image stack (B). *S.*Tm predominantly moves through areas with low fluorescence intensity. The tracks of the bacteria are shown in white. Fluorescent mucus is shown in red. (D) Quantification of the *S.*Tm swimming speed in the inner colonic mucus layer. The average *S.*Tm swimming speed during the traversal of the *RedMUC2*^{98trTg} mucus did not differ from the speed measured in the proximal colon of *villin-RFP* mice (compare with Fig. 4 B). The bars indicate the median and quartiles. (E) Quantification of the mCherry -MUC2 fluorescence at the location of swimming or trapped *S.*Tm from time-lapse microscopy data. Entrapped bacteria were preferentially located at sites with strong mCherry-MUC2 fluorescence. This could either be attributable to heterogeneous mucus densities or different adhesion properties between mucus of murine and human origin. Shown is the average fluorescence intensity beneath trapped *S.*Tm compared with swimming bacteria in the same image series. Each dot represents one time-lapse movie. Error bars delineate the mean ± SD. Statistics: Wilcoxon signed-rank test (non-parametric) testing whether the fluorescence ratio is different from 1.

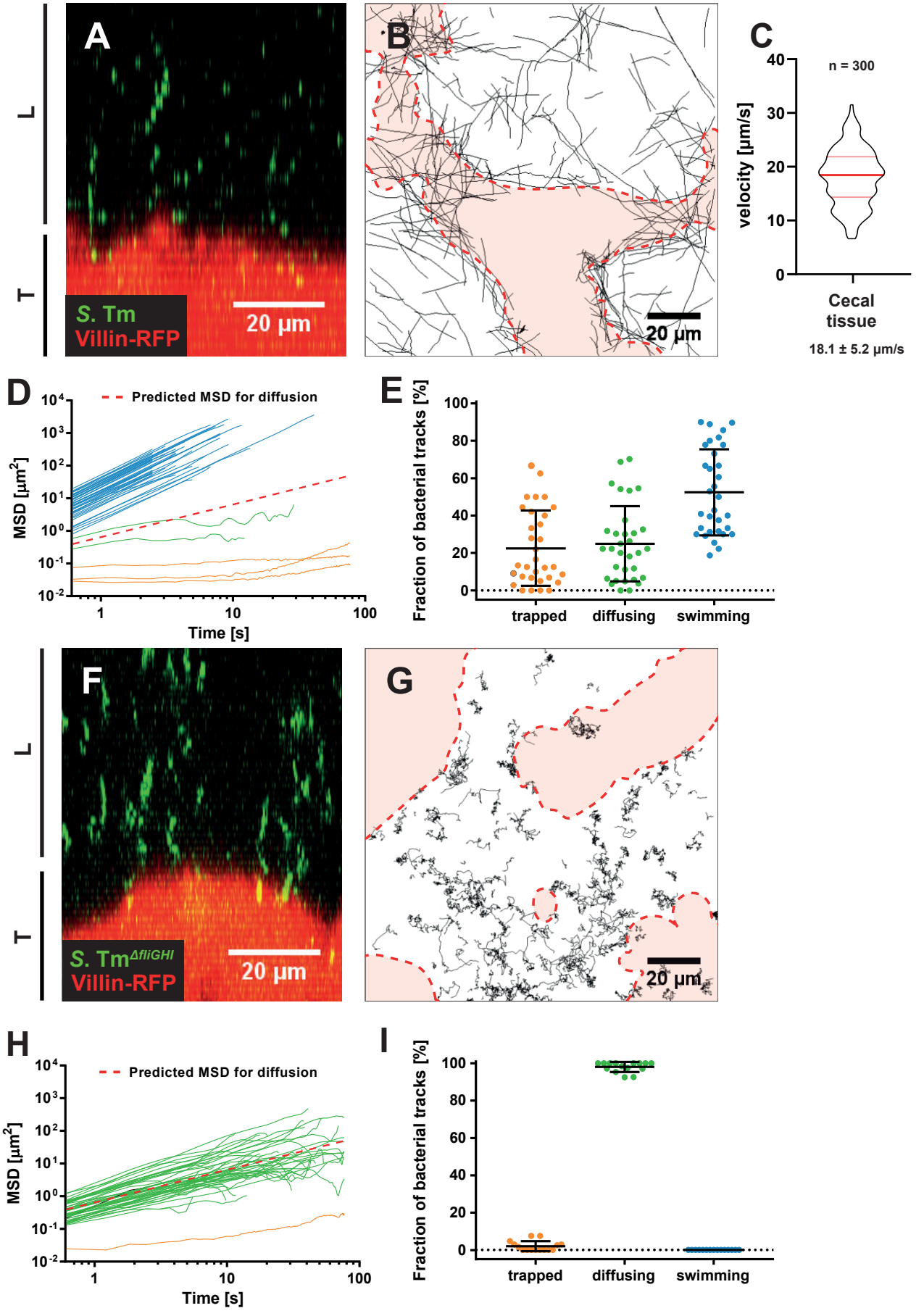
A
B
C
L
T
S. Tm
Villin-RFP
20 µm
n = 300
velocity [µm/s]
Cecal tissue
18.1 ± 5.2 µm/s
D
Predicted MSD for diffusion
MSD [µm²]
Time [s]
E
Fraction of bacterial tracks [%]
trapped
diffusing
swimming
F
G
S. TmΔfliGHI
H
I

Fig. S4, related to Fig. 5: The cecum tissue is easily accessible for *S.*Tm. (A - E) Cecal tissue samples were excised from untreated *villin-RFP* mice and mounted on a petri dish. After mounting, *S.*Tm^{GFP} was added onto the tissue and confocal image stacks were acquired. (A) Side-view of a confocal z-stack from the cecum after addition of *S.*Tm. Labels indicate the tissue (T) and the lumen / loose mucus (L). (B) Time-lapse imaging of the tissue surface in image stack (A). The tracks of the bacteria are shown in black. The red area marks the cecal tissue. See also Movie M7. (C) Swimming speed of actively moving *S.*Tm at the cecal tissue surface. Bars indicate the median and the quartiles. (D) Mean Squared Displacement (MSD) calculated from 50 random *S.*Tm tracks at the cecal tissue surface. The plot is color-coded for the motility phenotype of each track as in Fig. 1. (E) Trapped, diffusing and swimming *S.*Tm were quantified manually based on optical appearance of the tracks. Shown is the pooled data of three independent experiments. Each data point represents one image series. The error bars indicate the mean ± SD. (F - I) Cecal tissue samples were excised from untreated *villin-RFP* mice and mounted on a petri dish. After mounting, green fluorescent *S.*Tm$^{\Delta fliGHI}$ were added onto the tissue and confocal image stacks were acquired. (F) Side-view of a confocal z-stack from the cecum after addition of non-motile *S.*Tm$^{\Delta fliGHI}$. Labels indicate the tissue (T) and the lumen / loose mucus (L). (G) Time-lapse imaging of the tissue surface in (E). The tracks of the bacteria are shown in black. The red area marks the cecal tissue. (H) Mean Squared Displacement (MSD) calculated from 50 random *S.*Tm$^{\Delta fliGHI}$ tracks at the cecal tissue surface. The plot is color-coded for the motility phenotype of each track as in Fig. 1. (I) Trapped, diffusing and swimming *S.*Tm$^{\Delta fliGHI}$ were quantified manually based on optical appearance of the tracks. Shown is the pooled data of two independent experiments. Each data point represents one image series. The bars indicate the mean ± SD.

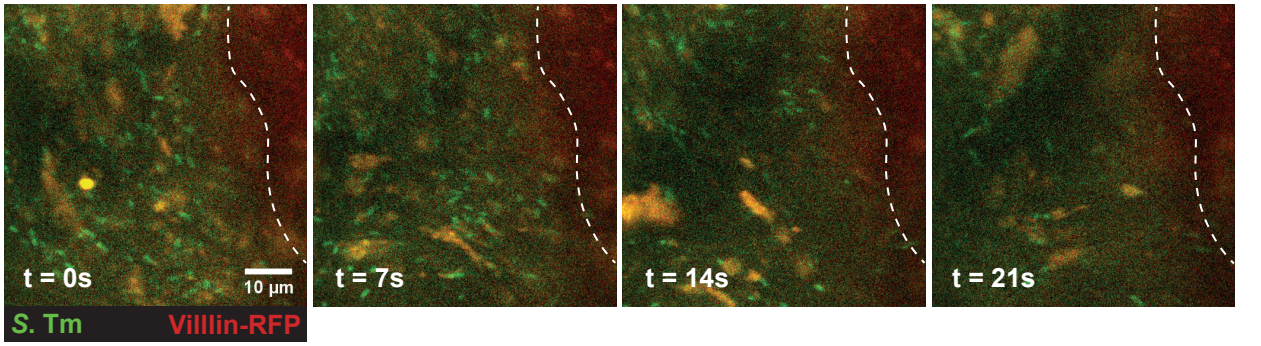
t = 0s
10 µm
t = 7s
t = 14s
t = 21s
S. Tm
Villlin-RFP

Fig. S5, related to Fig. 6: Light-induced heating of the samples leads to mixing of the intestinal content during intra-vital microscopy. *S.*Tm^{GFP} was injected into the cecal lumen of an anaesthetized *villin-RFP* mouse. *S.*Tm movement in the cecal lumen was tracked over time using two-photon microscopy. See also Movie M9. Fluorescent *S.*Tm^{GFP} are depicted in green. The border of the red fluorescent tissue is marked with the white dashed line. Auto-fluorescent food particles appear in orange. Thus, microscopy artefacts prevented more detailed analysis of the pathogen mucus interaction in the intact mouse gut.